A New Method for the Determination of the Geometries of Binary Transition Metal Complexes

JEREMY K. BURDETT

A simple model based on the interaction of ligand electron pairs and holes in the central metal charge distribution is used to rationalize the shapes of binary transition metal complexes. Only the orbital occupation numbers of the three highest d orbitals are important in determining the angular geometry, the deeper lying d orbitals being predominantly involved in π bonding. Depending upon how different the metal electronic charge distribution is from spherical, the overall geometry is sometimes intermediate between that demanded by these hole–pair forces and the structure with minimum ligand–ligand repulsion energy. Evidence is collected, suggesting that the first-order Jahn–Teller effect may be of secondary importance in determining these structures. The condition for successful use of the second-order Jahn–Teller effect is outlined.

Introduction

The geometries of transition metal complexes have, for some time, posed a problem for inorganic chemists. The VSEPR ideas of Sidgewick, Powell, Nyholm, and Gillespie,[1] so widely applied to main-group compounds, by experience are only readily applicable to transition metal systems containing a spherical electronic charge distribution (d^0, d^5, and d^{10}). In the presence of nonspherical situations the metal charge distribution is arbitrarily assumed to adopt an ellipsoidal shape which may sometimes be rationalized with the observed geometry.[2] The regular structures of some 18-electron d^6 and d^8 carbonyls and other complexes (*e.g.*, $Cr(CO)_6$ and $Fe(PF_3)_5$) are explained away by assuming that, since the metal d electrons are involved in π bonding with the ligands, they are ignored in the electron count determining the number of σ pairs. In this case the number of σ pairs surrounding the central metal is equal to the number of two-electron σ-donor ligands; octahedral and trigonal-bipyramidal (TBP) geometries are thus observed for $Cr(CO)_6$ and $Fe(PF_3)_5$, respectively.

One of the reasons for the slow development of theoretical ideas concerning the shapes of transition metal complexes has been the lack of good structural data. Few gas-phase geometries are known (the carbonyls and PF_3 complexes among them), compared to the data available for the main-group hydrides and halides for example. The solid-state structures of the transition metal halides are generally polymeric which makes it impossible to judge what the ideal "gas-phase" geometry would be in the absence of intermolecular interactions. Only for the d^0–d^4 hexafluorides MF_6 and some of the pentafluorides and the tetrachlorides of Ti and V (d^0 and d^1) are gas-phase structures of simple species readily known. However the synthesis in low-temperature matrices over the past few years of binary transition metal carbonyls and dinitrogen complexes, accompanied by excellent geometrical data, has alleviated this problem immensely. The novel structures of these $M(CO)_x$ and $M(N_2)_x$ species which contain less than 18 electrons present a challenge to the chemist who wishes to rationalize their shapes. The shapes of, for example, $M(CX)_4$ species vary from the tetrahedral $Ni(CO)_4$ through the D_{2d} or C_{3v} $Co(CO)_4$, C_{2v} $Fe(CO)_4$, and square-planar $Ni(CN)_4{}^{2-}$ structures to the octahedral "cis-divacant" $Cr(CO)_4$.

We present in this paper a simple scheme, based on overlap between ligand σ pairs and the holes in a nonspherically symmetrical charge distribution, to rationalize geometries either observed experimentally or predicted by recent molecular orbital calculations.[3]

The Perturbation Result and Molecular Bonding

The basis of the angular overlap method developed by Kettle,[4] Jorgensen,[5,6] and others is that the energy shift of an orbital ϕ_i on interaction with an orbital ϕ_j is approximately given by second-order perturbation theory as $\beta S_{ij}{}^2$ where S_{ij}

is the overlap integral between ϕ_i and ϕ_j. The parameter β is a measure of the strength of the interaction between the two and among other things is inversely proportional to the energy separation between the two unperturbed orbitals. A relationship of this type is also found by the completely equivalent method of ignoring terms in S^4 and higher powers in the binomial expansion of the secular determinant as is shown in the Appendix. Thus for main-group molecules of the type AY_n where a central A atom is surrounded by n σ ligands (Y), the total stabilization due to interaction of the orbitals of the central atom with the ligand σ orbitals will be

$$\Sigma(\sigma) = \beta_\sigma \sum_j n_j S^2 \left[A(\Gamma_j); \sigma(\Gamma_j) \right] \tag{1}$$

$A(\Gamma_j)$ and $\sigma(\Gamma_j)$ are respectively an orbital or group of orbitals located on the central atom and the ligand group of σ orbitals transforming under the jth representation of the molecular point group. n_j is the number of electrons occupying the bonding orbital(s) between A and Y which transform as Γ_j. In compounds of this type where all the bonding orbitals are filled (*e.g.*, NH_3) eq 1 may be rewritten as

$$\Sigma(\sigma) = 2\beta_\sigma \sum_j g_j S^2 \left[A(\Gamma_j); \sigma(\Gamma_j) \right] \tag{2}$$

where g_j is the degeneracy of the jth representation. The group overlap integrals S are dependent upon the angles the A–Y σ bonds make with an arbitary axis system and may be analytically expressed as a product of $S_\sigma(r)$ (where r is the A–Y bond length, held constant) and functions of the spherical harmonics $Y_{l,m}(\theta, \phi)$. The angular geometry exhibited by the AY_n molecule will then be determined by the maximum value of the term $\Sigma(\sigma)$ in eq 2, since this represents the maximum overall angular A–Y stabilization. This geometry will be independent of the parameter β and the values of the n_i. It has been noted previously[7-9] that the minimum-energy molecular orbital structure is that of maximum central atom orbital–occupied ligand orbital overlap as is also suggested by eq 2. These maximum overlap structures correspond to the ones predicted by the VSEPR approach given the total number of σ pairs and surprisingly may be evaluated within the confines of simple Hückel theory.[7] Inclusion of π bonding between A and Y leads to an analogous term $\Sigma(\pi)$, evaluated in a fashion similar to eq 1

$$\Sigma(\pi) = \beta_\pi \sum_j n_j S^2 \left[A(\Gamma_j); \pi(\Gamma_j) \right] \tag{3}$$

Because A–Y π overlap integrals are generally smaller than their σ counterparts, $\Sigma(\pi)$ is expected to be smaller than $\Sigma(\sigma)$ and therefore exert a correspondingly smaller influence on molecular geometry. In the VSEPR method π interactions are generally ignored in determining the gross angular arrangement of the ligands. Equations 2 and 3 tell us nothing very new about the factors influencing the molecular geometries

of main-group compounds but set the stage for discussion of transition metal complexes.

We shall assume for simplicity that the geometry of these species is determined predominantly by interactions between the ligand orbitals and the metal nd orbitals. The $(n + 1)s$ orbital closest to the metal nd orbitals is spherically symmetrical. The overlap integrals of eq 2 involving it will therefore be isotropic and of no importance in this scheme and therefore to first order at least in determining the *angular* molecular geometry. The vital difference between the main-group AY_n structures and the binary transition metal MY_n ones is that on a molecular orbital basis the M–Y σ-antibonding orbitals (predominantly metal nd) are generally occupied (d^1–d^{10}). Thus the total σ stabilization becomes

$$\Sigma(\sigma) = \beta_\sigma \sum_j (2g_j - n_j)S^2 \, [\mathrm{d}(\Gamma_j); \sigma(\Gamma_j)] \tag{4}$$

where n_j is now the number of antibonding M–Y electrons in the d orbitals of the g_j degenerate jth representation. This is assuming that the destabilization afforded by an electron in an M–Y σ-antibonding orbital is equal to the stabilization exerted by an electron in the corresponding bonding orbital. Equation 4 may be simply rewritten as

$$\Sigma(\sigma) = \beta_\sigma \sum_j h_j S^2 \, [\mathrm{d}(\Gamma_j); \sigma(\Gamma_j)] \tag{5}$$

where h_j is the number of holes in the d-orbital manifold. Hence for the case of σ-donor ligands, the geometry with the maximum stabilization predicted by eq 5 is that where there is greatest overlap between the holes in the metal charge distribution with the occupied ligand σ orbitals, *i.e.*, maximum coincidence of regions of high electron density (pairs) with those of low electron density (holes). The *overall* equilibrium geometry will then be a compromise between the structure demanded by maximum hole–pair overlap and that reached by minimizing interactions between the ligands. These will consist of nonbonded interactions and the forces of interaction between the ligand pairs so important in the VSEPR approach. We shall call these interactions ligand–ligand interactions. The hole–pair forces are expected to be the larger of the two since they derive from directly bonded rather than nonbonded interactions. Some idea of the relative importance of these two types of interaction may be obtained by comparing the angle bending force constants of $Ni(CO)_4$ and $Cr(CO)_6$. The tetrahedral geometry of the d^{10} nickel complex is determined by ligand–ligand interactions; $\Sigma(\sigma)$ of eq 5 is identically zero since there are no holes in the d-orbital manifold. By way of contrast the $Cr(CO)_6$ molecule is held in the octahedral geometry by a combination of these forces and the hole–pair interactions of eq 5. As a result the chromium force constant is several times larger than its nickel counterpart.[10]

If filled π orbitals are included on the ligands, then a term $\Sigma(\pi)$ has to be added to $\Sigma(\sigma)$, and the total stabilization now becomes a weighted mean of that determined by overlap of σ pairs and metal holes and that determined by overlap of π pairs and metal holes. To a good approximation however the π term may probably be neglected in determining the angular molecular geometry (*vide supra*). It is interesting to note however that if empty π^* orbitals are available on the ligands, then, ignoring the filled ligand π type orbitals

$$\Sigma(\pi) = \beta_\pi \sum_j n_j S^2 \, [\mathrm{d}(\Gamma_j); \pi^*(\Gamma_j)] \tag{6}$$

instead of the corresponding hole equation. Thus in the case of a π donor (filled π orbitals reasonably close to the d orbitals) the maximum π stabilization arises through overlap of π pairs with metal holes, whereas for a π-acceptor ligand, the maximum stabilization occurs for the geometry where there is greatest overlap between the filled (or partially filled) metal d orbitals with holes in the ligand π^* orbitals.

One important property of the Σ functions that we shall find useful, is that, $\Sigma(\sigma)$ for example is independent of angle if all the d orbitals with nonzero σ interactions contain equal numbers of electrons, *i.e.*, zero, one, or two electrons. This is nothing more than a specific example of the generalized Unsold theorem (see for example ref 11) which states that the function $\Sigma\phi_j^2$ is invariant under all operations of the point group for which the ϕ_j form the basis of an irreducible representation, *i.e.*, is spherically symmetrical. For example the configuration t_2^3 is spherically symmetrical in the tetrahedral point group since the function $(xy)^2 + (xz)^2 + (yz)^2$ is invariant under all rotations and thus all rotations of the point group T_d. (The only nonzero metal–ligand σ interactions in this point group are of species t_2.) On the occasion when the function $\Sigma(\sigma)$ (neglecting $\Sigma(\pi)$) is independent of angle due to the correct occupation numbers of the d orbitals, then the resultant structure is determined purely by VSEPR type interactions between the ligand pairs. Thus, whereas for main-group molecules the VSEPR structure and the arrangement of maximum overlap of eq 2 correspond to the *same* angular disposition of the ligands, for the transition metal series, the VSEPR geometries and those predicted by eq 5 are not necessarily the same.

Determination of the Equilibrium Geometry

It has been noted in the previous section that π interactions are probably very much less important than their σ counterparts. We need then only to determine the geometry which will give the maximum value of $\Sigma(\sigma)$ in eq 5 with a given d-electron configuration. In general the deeper lying d orbitals will be mainly concerned with π interactions with the ligands, whereas the higher lying orbitals will be mainly concerned with the much more energetic and structurally more important σ interactions. For the five-coordinate TBP structure, the four-coordinate tetrahedral structure, and the three-coordinate trigonal (D_{3h}) structure for example the lowest pair of d orbitals in each case are solely concerned with π interactions. In all geometries where the ligands lie at the vertices of an octahedron, the lowest three orbitals are purely involved in π bonding. In our considerations of the molecular geometry problem we shall therefore ignore the presence of any holes in the lowest two d orbitals since these will be structurally impotent and focus our attention on the holes in the three highest energy d orbitals. Parenthetically we note that in this observation lies the explanation of Gillespie's[2] remark "when the number of d electrons is small, typically one to three, the interaction of the d shell with the bonding electrons is generally weak and any distortion of the arrangement of bonding pairs appears to be negligible or at least too small to be seen." In d^5 $V(CO)_6$ and several d^0–d^4 MF_6 species, where all the σ-antibonding orbitals are empty, the VSEPR octahedral geometry is therefore observed. Where the purely π-bonding t_{2g} set of orbitals do contain holes, small distortions of the dynamic type are often observed but no large-scale structural distortions comparable to the ones we are about to describe. Since we thus surmise that the term $\Sigma(\pi)$ is much less important than $\Sigma(\sigma)$, the conclusions will be applicable to all binary metal–ligand systems containing monodentate ligands, irrespective of whether the ligands are π donors or acceptors.

The sum total stabilization of the ligand σ orbitals (and hence approximately the sum total destabilization of the metal d orbitals) can be readily shown from eq 5 to be[5] equal to $n\beta_\sigma S_\sigma^2$ where n is the number of ligands and S_σ is the overlap integral between a ligand σ orbital and one lobe of the d_{z^2} orbital. Thus the total d orbital destabilization in a four-coordinate tetrahedral complex is $4\beta_\sigma S_\sigma^2$. Since in this geometry the total metal–ligand σ interactions are contained in the t_2 representation, the separation between the t_2 and e sets of d orbitals is then $^4/_3\beta_\sigma S_\sigma^2$. The total stabilization energy
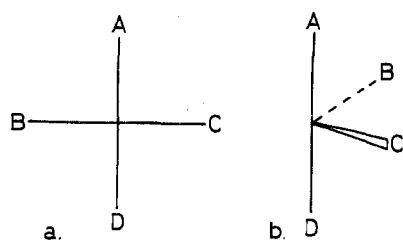
Figure 1. The two possible geometries for four-coordinate complexes based on the octahedron: (a) the square plane and (b) the cis-divacant (or double-tailed T) structure.

Figure 2. Four-coordination: (a) overlap of four ligand σ orbitals with the lobes of $d_{x^2-y^2}$ in the square-planar geometry; (b) overlap of four ligand σ orbitals with d_{z^2} in the cis-divacant geometry (for the sake of clarity the ligand "lobes" are not shown).

$\Sigma(\sigma)$ from eq 5 for a d^8 system (d-orbital occupation numbers 22220) is thus $2.67\beta_\sigma S_\sigma^2$. However, it is readily appreciated that this geometry does not give rise to the maximum stabilization required by eq 5. This will occur for maximum ligand pair–hole overlap and as will be shown below, but may be readily visualized here, is found for the configuration where the ligand pairs overlap the lobes of the $d_{x^2-y^2}$ orbital, *i.e.*, the square-planar geometry. Here the destabilization of the $d_{x^2-y^2}$ orbital is found to be $3\beta_\sigma S_\sigma^2$ and thus that of the d_{z^2} orbital is $\beta_\sigma S_\sigma^2$. The total stabilization energy for the 22220 configuration in the square-planar geometry is thus $6\beta_\sigma S_\sigma^2$, sizably larger than $\Sigma(\sigma)$ for the tetrahedral structure. In agreement with these ideas, although d^{10} Ni(CO)$_4$ is tetrahedral, the two low-spin d^8 systems AuCl$_4^-$ and Ni(CN)$_4^{2-}$ are both square planar. For the d^{10} structure of course $\Sigma(\sigma) = 0$ for all angular geometries and the structure is determined purely by VSEPR forces.

For the configuration 22200, holes are now present in the two highest energy orbitals. As noted above these two orbitals will contain the total σ interaction for a geometry where the ligands occupy the vertices of an octahedron. This condition is satisfied for both the square-planar and cis-divacant structures of Figure 1, both of which have values of $\Sigma(\sigma) = 8\beta_\sigma S_\sigma^2$ for the configuration 22200. We need to go a little further than eq 5 to decide which of the two structures will be of lower energy. By considering terms in S^4 we can readily show (Appendix) that the cis-divacant structure is favored relative to the square-planar one for this electronic configuration. The preference for orthogonal ligand geometries is seen in a tabulation of C–M–C bond angles in substituted metal carbonyls.[4] Particularly noticeable are M(CO)$_3$ groups with pseudocylindrical symmetry where C–M–C bond angles of *ca.* 90° are seen. In less symmetric structures the bond angles are close to but usually greater than 90°.

Four-Coordination

We start with this coordination number since most of the main points of the method are readily illustrated in the rationalization of the five different observed geometries for these systems. The VSEPR structure for four ligand pairs is a regular tetrahedron and this structure is expected and observed for the spherically symmetrical d^{10} Ni(CO)$_4$ molecule and Ni group four-coordinate N$_2$ and CO compounds.[12] Deviations from this geometry, where ligand pair–ligand pair repulsions are minimized, will arise through competing ligand pair–metal hole interactions described by eq 5. If the occupation numbers of the lowest pair of orbitals are not important as we have suggested above, then the tetrahedral structure should be observed for all systems with a 111 or 222 occupation of the higher lying orbitals. (This therefore includes the configurations 21111 and 22111, and indeed high-spin d^6 and d^7 tetracarbonyls were found to be tetrahedral in our previous calculations.)[3] If the spherically symmetric situation 222 or 111 is destroyed by removing one or two electrons from the highest energy orbital to give the electron configurations 220, 221, or 110 (these are the orbital occupation numbers of the three highest energy d orbitals), then the geometry where
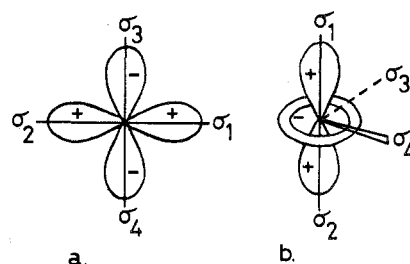
maximum ligand–hole overlap occurs is not the tetrahedral structure but the square-planar arrangement of Figure 2a as suggested above. In this geometry the $d_{x^2-y^2}$ orbital is the highest energy orbital. An alternative structure might be the "cis-divacant" octahedral structure (C_{2v}) of Figure 2b where two ligands directly overlap the lobes of the d_{z^2} orbital and the other two lie perpendicular to it. In this geometry, the highest energy d orbital is d_{z^2} and thus the holes must appear here rather than in the more stable $d_{x^2-y^2}$ orbital. This axis system, based on that of the octahedron, is chosen in preference to one where the z axis contains the twofold axis. The advantage of the system used here is that only two group σ-overlap integrals (with d_{z^2} and $d_{x^2-y^2}$) are nonzero and these belong to different irreducible representations. (Under the C_{2v} point group, where the z axis contains the twofold axis, d_{z^2} and $d_{x^2-y^2}$ both transform as a_1 and would thus mix together.) We may readily show the structure of Figure 2a to be energetically favored by evaluation of the S^2 function in eq 5. For the structure of Figure 2b the group overlap integral of the four ligands with the d_{z^2} orbital is given by the overlap of the function

$$\phi_{z^2} = \frac{1}{10^{1/2}}(2\sigma_1 + 2\sigma_2 - \sigma_3 - \sigma_4)$$

with the d_{z^2} orbital. This is equal to $(1/10^{1/2})(5S\sigma)$, where S_σ is the overlap integral of a ligand σ orbital located on the z axis with one lobe of the d_{z^2} orbital. (The overlap integral of σ_3 or σ_4 with the "collar" of d_{z^2} is $^1/_2S_\sigma$.) Thus $S^2 = 2.5S_\sigma^2$. For the structure of Figure 2a the group overlap integral of the four ligands with the $d_{x^2-y^2}$ orbital is given by the overlap of the $d_{x^2-y^2}$ orbital with the function

$$\phi_{x^2-y^2} = {}^1/_2(\sigma_1 + \sigma_2 - \sigma_3 - \sigma_4)$$

and is equal to $3^{1/2}S\sigma$. (The overlap integral between a ligand σ orbital and one lobe of a $d_{x^2-y^2}$ orbital is $(3^{1/2}/2)S\sigma$.) S^2 for this structure then becomes $3S_\sigma^2$, *i.e.*, a more stable arrangement than that of Figure 2b. For the tetrahedral geometry, S^2 is a mere $1.3S_\sigma^2$. Thus the square-planar geometry is observed for diamagnetic (low-spin) Ni^{II} and Au^{III} species as described above. Creation of holes in the two highest energy metal d orbitals (200, 211, or 100) leads to a slightly more complex situation. In order to elucidate the geometry with the largest value of $\Sigma(\sigma)$ we must remember that the two holes must occupy the two highest energy d orbitals of that geometry. As noted above this will be an arrangement where the ligands occupy the corners of an octahedron and of the two possible structures, the cis-divacant one should be favored. Creation of three holes gives the spherically symmetric configuration 000 which of course leads to the VSEPR-determined tetrahedral geometry.

For the d^6 species Cr(CO)$_4$ (200) the cis-divacant geometry as been experimentally observed[13] whereas the d^8 species Fe(CO)$_4$ (211) has been shown[14] to exhibit a C_{2v} structure with bond angles of $\sim$120 and $\sim$140°. Most high-spin Ni^{II} complexes are distorted from the strictly regular tetrahedral

Jeremy K. Burdett

Table I. Values of $\Sigma(\sigma)$ for Different Four-Coordinate Structures (Units of $\beta_\sigma S_\sigma{}^2$)
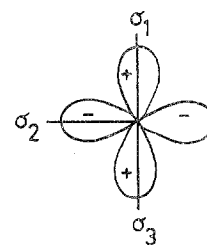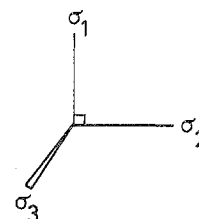
	Square planar	Tetra-hedral	Cis di-vacant	Obsd geometry
222	0	0	0	Tetrahedral Ni⁰
221	3.0	1.3	2.5	D_{2d}, D_{4h} sq-planar Cu^{II}
220	6.0	2.7	5.0	Sq-planar Ni^{II}
210	7.0	4.0	6.5	
211	4.0	2.7	4.0	C_{2v} dist. tetrahedral Ni^{II}
200	8.0	5.3	8.0	Cis-divacant Cr⁰
111	4.0	4.0	4.0	Tetrahedral Co^{II}
110	7.0	5.3	6.5	
100	8.0	6.7	8.0	
000	8.0	8.0	8.0	Tetrahedral TiCl₄

Figure 3. Three-coordination: Overlap of three ligand σ orbitals with the lobes of $d_{x^2-y^2}$ in the T geometry (for the sake of clarity the ligand "lobes" are not shown).

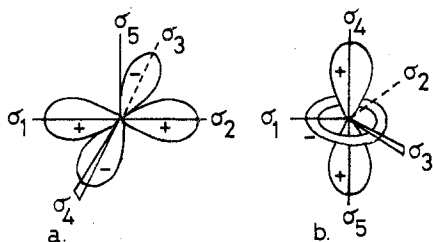**Figure 4.** Three-coordination: The C_{3v} geometry for three metal ligand bonds at right angles to one another.

T_d geometry to give a similar C_{2v} or C_s structure. These structures are intermediate between the VSEPR tetrahedral geometry (angles 110, 110°) and the hole–pair determined structure (angles 90, 180°). This observation may be understood in the following way. The driving force from the tetrahedral geometry will depend qualitatively on the extent of the deviation from the spherically symmetric 222 or 111 configurations. Thus the angular distorting forces from the VSEPR geometry are expected to be larger for the 200 and 100 configurations than for the intermediate 211. This is seen above in the equilibrium Cr(CO)₄ and Fe(CO)₄ geometries. In the former (200) the geometry is determined by the hole–pair interactions of eq 5; in Fe(CO)₄ however the overall geometry is a compromise between the directly bonded hole–pair forces and the nonbonded ligand–ligand forces. These data give us an idea as to the size of the ligand–ligand forces in terms of the stabilization energy of eq 5. For the configuration 200 the total value of $\Sigma(\sigma)$ for the cis-divacant geometry is $8\beta_\sigma S_\sigma{}^2$ and for the tetrahedral geometry $5.3\beta_\sigma S_\sigma{}^2$, a difference of $2.7\beta_\sigma S_\sigma{}^2$. For the 211 configuration the energy difference is half of this value, *i.e.*, $1.3\beta_\sigma S_\sigma{}^2$. This energy difference is thus insufficient to overcome the increase in ligand–ligand repulsion energy on moving from the tetrahedral geometry (bond angles 110°) to the cis divacant structure. Support for these ideas comes from our previous molecular orbital calculations.[3] For the 220 and 110 configurations the square-planar geometry is calculated to have the lowest energy. For 200 and 100 the cis-divacant structure is favored. For 211 the C_{2v} Fe(CO)₄ geometry is predicted with bond angles close to those experimentally observed. (The angles of the calculated geometry may be slightly varied of course by choosing a different parametrization in the molecular orbital method.) For 221 a D_{2d} structure with bond angles of 132° (*i.e.*, halfway between square planar and tetrahedral) was found. Experimentally there is some controversy[15,16] over the geometry of d⁹ Co(CO)₄ which has this configuration; both D_{2d} and C_{3v} structures have been claimed. It is certainly neither tetrahedral nor square planar. Complexes containing Cu^{II} give us more definitive data concerning the shapes of four-coordinate complexes with the 221 electronic configuration. Both square-planar geometries[17] (*e.g.*, CuCl₄²⁻ in (NH₄)₂CuCl₄) and squashed tetrahedra of the D_{2d} point group (*e.g.*, CuCl₄²⁻ in Cs₂CuCl₄) have been observed[18] in agreement with our ideas.

For the d⁷ 210 electron configuration the square-planar geometry is predicted but no experimental data are available. (Four-coordinate Co^{II} (d⁷) species are tetrahedral in agreement with the high-spin configuration 111 for this system.) Table I shows the calculated values of $\Sigma(\sigma)$ for the various structures, as a function of electron configuration, and some examples of the observed geometries.

Two-Coordination

The VSEPR geometry is of course the linear arrangement. This geometry should then be favored for d¹⁰ species (222) by virtue of VSEPR forces since $\Sigma(\sigma) = 0$ as has been ex-

perimentally confirmed[12] for the Ni, Pd, Pt, N₂, and CO complexes and several two-coordinate compounds of Cu^I. For this linear structure the total σ interaction is contained in the $\sigma_g{}^+$ representation. The single d orbital of this species is thus destabilized by $2\beta_\sigma S_\sigma{}^2$ and this structure should therefore be observed for the 220 configuration and indeed for the 221 system. For the 200 configuration the linear and bent geometries (L–M–L angle 90°) become equally favored by eq 5 but our previous arguments would suggest that the bent geometry is more stable. Thus for the electronic configurations 200 and 100 the theory outlined in this paper predicts that the 90° geometry should be seen, for 211 a structure somewhere between the linear and 90° geometries should be observed, and for all others the linear arrangement is expected. Apart from the d¹⁰ systems, the only available experimental data concern the d⁷ (210) species Co^{II}N(SiMe₃)₂ which in agreement with theory is linear.[19]

Three-Coordination

The VSEPR geometry for these species is the flat D_{3h} structure. This geometry has been experimentally observed for d¹⁰ Ni(CO)₃ and other tris N₂ or CO Ni-group systems and d¹⁰s¹ Ni(CO)₃⁻ [20] and Cu(CO)₃.[21] Creation of a hole in the highest energy d orbital (220 or 110) leads to an in-plane distortion to give a planar T-shape structure (Figure 3) where the hole–pair overlap is a maximum with the $d_{x^2-y^2}$ orbital ($S^2 = {}^9/_4S_\sigma{}^2$). This is a situation very similar to that observed with a single hole in the four-coordination case. After the discussion of the previous section, the configuration 221 is expected to give rise to a smaller distortion from D_{3h}. Our previous molecular orbital calculations gave[3] values of $\alpha \approx 70°$ for 220 and 110 and $\sim 150°$ for 221 in agreement with these ideas. Two holes in the top two d orbitals should lead analogously to a structure based on the cis-divacant structure of the four-coordinate complex. If either A or D is removed from Figure 1b a C_{3v} structure with all bond angles between the ligands of 90° is achieved (Figure 4). This geometry has a droop angle from planar (D_{3h}) of about 32°. Our previous molecular orbital calculations[3] arrived at C_{3v} structures with droop angles of about 30° (for 200 and 100) and 17° for the less dynamic 211 structure. Experimentally Cr(CO)₃ (200) is found[13] to have a droop angle of $\sim 25°$ whereas Fe(CO)₃ (211) is found[22] to have an angle of $18 \pm 3°$ in good agreement with these ideas. The T-shape structure is predicted for the 210 species but no experimental information is available for

Table II. Values of $\Sigma(\sigma)$ for Different Three-Coordinate Structures (Units of $\beta_\sigma S_\sigma{}^2$)

	T shape	Planar D_{3h}	Pyramidal (90°)	Obsd geometry
222	0	0	0	D_{3h} Ni°, Ni⁻
221	2.25	1.125	1.5	
220	4.50	2.25	3.0	
210	5.25	3.375	4.5	
211	3.00	2.25	3.0	C_{3v} Fe°
200	6.0	4.50	6.0	C_{3v} Cr°
111	3.0	3.0	3.0	
110	5.25	4.125	4.5	
100	6.0	5.25	6.0	
000	6.0	6.0	6.0	

Table III. Values of $\Sigma(\sigma)$ for Different Five-Coordinate Structures (Units of $\beta_\sigma S_\sigma{}^2$)

	Trigonal bipyramid	Square pyramid	Diff
222	0	0	0
221	2.75	3	0.25
220	5.5	6	0.5
210	6.625	8	1.3
211	3.875	5	1.2
200	7.75	10	2.25
111	5	5	0
110	7.75	8	0.25
100	8.875	10	1.3

Figure 5. Five-coordination: (a) overlap of five ligand σ orbitals with $d_{x^2-y^2}$ in the square-pyramidal geometry; (b) overlap of five ligand σ orbitals with d_{z^2} in the trigonal-bipyramidal geometry (for the sake of clarity the ligand "lobes" are not shown).

three-coordinate species with this configuration. For systems with spherically symmetric charge distributions the D_{3h} structure is observed as noted above for d¹⁰ Ni(CO)₃. Here $\Sigma(\sigma) = 0$. This planar structure is also seen[23] for the d⁵ species Fe^III[N(SiMe₃)₂]₃ as befits a 11111 high-spin configuration. Table II lists the total calculated stabilizations from eq 5 for each of the possible geometries. Unfortunately the number of well-defined three-coordinate complexes is small.

Five-Coordination

The equilibrium geometries for the tri- and tetracarbonyls containing a hole in one d orbital were based upon maximum overlap of the ligand σ pairs with the lobes of a $d_{x^2-y^2}$ orbital. With five ligands the arrangement where four of the pairs overlap these four lobes and the fifth ligand does not interact with the hole is the square-pyramidal (SPY) C_{4v} structure and is favored energetically compared to the D_{3h} structure where all the ligands may overlap with the (now highest energy) d_{z^2} orbital (Figure 5). This is contrary to experience since d⁸ Fe(CO)₅ with one hole has an experimentally determined D_{3h} and not C_{4v} structure. The two are indeed close together in energy as evidenced by rapid axial–equatorial ligand exchange.[24] One of the suggested mechanisms of this process occurs *via* distortion of the D_{3h} geometry to C_{4v} and back again (the Berry mechanism). This fact is underlined by comparing the smaller calculated energy difference for 220 between the two structures (Table III) than between the tetrahedral and square-planar structures for the four-coordinate case (Table I). Indeed for almost any electronic configuration there is quite a small calculated energy difference between the TBP and SPY geometries. In fact the true energy differences will be even smaller since the calculated stabilization for the SPY structure in Table III is for the arrangement where all L–M–L bond angles are 90 or 180°. The actual ML₅ molecule will have a nonzero "droop" angle with a concurrently smaller stabilization. Dependent upon the size of $\gamma\sigma$ (see Appendix), inclusion of the quartic term might even tip $\Sigma(\sigma)$ in favor of the TBP structure for 220.

This energy difference may also be compared to the difference in energy between the tetrahedral and cis divacant structures of $1.3\beta_\sigma S_\sigma{}^2$ for the 211 tetracoordinated case. In this circumstance the observed Fe(CO)₄ geometry was halfway

between that determined by ligand–ligand repulsion effects and that demanded by the eq 5. In the more crowded situation of the five-coordinate structure the ligand–ligand terms should be even larger. This closeness in $\Sigma(\sigma)$ for the two structures implies that steric and crystal effects will be important in deciding the overall geometry and in many solid-state structures the observed disposition of the atoms is intermediate between the two (C_{2v}). It is noted that the largest stabilization of the C_{4v} geometry relative to TBP is found for the 200 configuration. d⁶ Cr(CO)₅ (200) has been found[25-27] to have this geometry whereas Fe(CO)₅ is TBP. Similarly the C_{4v} geometry has been observed for the d⁷ (210) system Re(CO)₅.[21] Some of the salient points of the photochemistry of the d⁶ pentacarbonyl may be explained[28] using a TBP excited state (110).
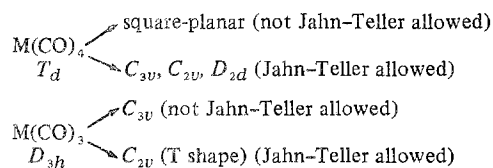
Six-Coordination

The hypothetical 222 (22-electron) molecule should exhibit the regular octahedral VSEPR structure. The presence of one hole in the d-orbital manifold will still result in the octahedral geometry since maximum ligand–hole overlap between the $d_{x^2-y^2}$ or d_{z^2} orbitals occurs for this structure. The presence of two holes will also require the octahedral arrangement. This geometry is observed for d⁶ Cr(CO)₆. For V(CO)₆ a hole is also present in the t₂g (purely π-bonding) d orbitals. Experimentally no static structural distortion has been observed, purely a dynamic one commensurate with the expected sizes of $\Sigma(\pi)$ compared to $\Sigma(\sigma)$. The model thus predicts octahedral angular geometries for all hexacoordinated systems, irrespective of the number of d electrons, and is confirmed by the observation of basically octahedral geometries for d⁰–d⁴ MF₆ species, V(CO)₆ and Cr(CO)₆. Our remarks however do not preclude a distortion to, *e.g.*, D_{4h} *via* contraction or extension of two axial ligands; our model assumes equal lengths for all M–L bonds. For a d⁸ (220) or d⁹ (221) system, for example, with a hole in the $d_{x^2-y^2}$ orbital and with a nonzero equatorial bond strength, from eq 5 we find a zero bond strength between the metal and axial ligands. This point has interesting consequences when applied to Cu^II (d⁸) systems (Jahn–Teller unstable) and Ni^II (d⁸) systems (square-planar–octahedral isomerization).[29]

For a system containing holes in two orbitals (*e.g.*, 200) the holes appear in d_{z^2} as well as $d_{x^2-y^2}$ and thus all bond lengths should be equal.

Connection with the Jahn–Teller Theorems

In several cases the predicted Jahn–Teller instability of certain structures based on the symmetry species of the electronic state concerned is not found either by experiment as a distorted equilibrium geometry or by earlier molecular orbital calculations.[3] These occurrences however are always concerned with the presence of holes in purely π-bonding manifolds and represent the smaller structural effect of $\Sigma(\pi)$ compared to $\Sigma(\sigma)$. Often, of course, dynamic effects are observed. More significant is the fact that some of the distortions observed from the symmetric ligand–ligand repulsion structures are not allowed[30] as distortions under the first-order

Jahn–Teller theorem for *any* species of electronic state. For example

$M(CO)_4$ — square-planar (not Jahn–Teller allowed)
T_d — C_{3v}, C_{2v}, D_{2d} (Jahn–Teller allowed)

$M(CO)_3$ — C_{3v} (not Jahn–Teller allowed)
D_{3h} — C_{2v} (T shape) (Jahn–Teller allowed)

One conclusion is that the structural effect of the Jahn–Teller theorem can be viewed as a special case of the hole–pair approach in situations where orbital degeneracy occurs. This point is especially interesting since the Jahn–Teller effect itself is often regarded from the viewpoint of holes appearing in spherically symmetric charge distributions.

Sometimes the observed "Jahn–Teller" distortion from the symmetrical structure is larger than intuition would lead one to expect.[14] This also suggests another force operative in determining the geometries of these systems. (In this light, it is interesting to recall the comment of Kettle and Jotham[30] that it is possible that no true Jahn–Teller distorted structure has been observed.) Thus whereas all the distortions from the symmetric VSEPR-determined structures can be rationalized by considering the forces between the holes and ligand pairs *irrespective* of the species of the ground electronic state,[31] the Jahn–Teller contribution is restricted to those systems where the electronic ground state is orbitally degenerate and may be small by comparison. Our point is therefore that the importance of the Jahn–Teller effect in determining molecular geometries (as distinct from small dynamic effects) has been very considerably overemphasized in the past. Interestingly only small (dynamic) "Jahn–Teller" effects are observed in orbitally degenerate systems when $\Sigma(\sigma)$ is angle independent (*e.g.*, $V(CO)_6$, ReF_6) and the angular geometry is controlled by VSEPR and $\Sigma(\pi)$ forces. Whereas the size of the Jahn–Teller distortion energy is not readily calculable, the opposite is true of $\Sigma(\sigma)$ for a particular geometry and electronic configuration. This makes the present method a more powerful approach for determining molecular shapes.

The structural predictions[8,32,33] of the second-order (pseudo) Jahn–Teller effect are also found generally to give rise to experimentally unconfirmed geometry changes. For example the reference geometry for the three-coordinate system is the trigonal plane and the d orbitals are split into three sets, e″, a_1', e′ (deepest lying first). The structural predictions of the theory suggest transition densities of species e″ (*i.e.*, no distortion) for low-spin d^1–d^4 systems; this arises through the promotion of an electron from the e″ to a_1' orbital. For d^5–d^9 systems the transition a_1' to e′ is possible leading to a predicted distortion of species e′, *i.e.*, to a T-shaped molecule. This is certainly not experimentally observed for the d^6 and d^8 chromium and iron tricarbonyls. On closer examination we would not expect the second-order Jahn–Teller theorem to predict the angular geometries of these d^1–d^9 systems although it has been used to rationalize the magnitude and sign of various stretching vibrational constants in metal carbonyls.[34] The wave function of the ground state $|0\rangle$ becomes on distortion

$$|0\rangle' = |0\rangle + q_i \sum_m{}' \frac{|\langle 0|\mathcal{H}_i|m\rangle|^2}{E_m{}^{(0)} - E_0{}^{(0)}} |m\rangle \qquad (7)$$

$\mathcal{H}_i$ is the first derivative of the electronic Hamiltonian with respect to the normal coordinate q_i and the admixture of $|m\rangle$ into the ground state on distortion *via* q_i depends upon the overlap between $|0\rangle$ and $|m\rangle$ and on the zeroth-order energy separation between them. As a result $|0\rangle$ is depressed and $|m\rangle$ raised in energy on distortion by this interaction. For the 200 system for example although the highest energy orbital *may* be destabilized during a particular distortion *via* eq 6, no

information is obtained concerning the net destabilization of the *two* highest orbitals which from eq 5 is the energy term we need to consider. These remarks, however, suggest that the pseudo Jahn–Teller effect should be applicable to low-spin d^8 and d^9 systems (220, 221) where only one orbital is vacant. For three-coordinate systems as noted above an e′ distortion is predicted. This is equivalent to the T-shape distortion from D_{3h} demanded by eq 5 for these systems. For such $^1E'(d^8)$ and $^2E'(d^9)$ however this e′ vibration also relieves the orbital degeneracy *via* the first-order Jahn–Teller effect predicted to occur here but in view of our discussion above this may not be important. For the four-coordinate tetrahedral system 220 the singlet manifold contains $^1A_1$, ^1E, and $^1T_2$. The $^1A_1$ state lies to higher energy than the other two states which are isoenergetic. The transition $^1T_2 \rightarrow {}^1A_1$ leads to a transition density of species t_2. The bending vibration of this species sends the tetrahedral into a C_{2v} geometry. The transition $^1E \rightarrow {}^1A_1$ on the other hand leads to a transition density of species e which sends the tetrahedral geometry into the square-planar structure predicted by eq 5.

For the five-coordinate TBP structure the pseudo Jahn–Teller active vibration is of species e′ (transition from e′ to a_1' orbital). This vibration converts the D_{3h} to the C_{4v} geometry. The second-order Jahn–Teller predicted geometry is thus also the one found to be of lowest energy by evaluation of eq 5. The other situation where the structural predictions of the pseudo Jahn–Teller effect should be valid is where there are no d electrons at all. Here there are no electrons in metal–ligand antibonding orbitals and the interaction between the central atom and ligands will be described by eq 2 rather than eq 5. This discussion should be sufficient to warn against a straightforward application of the pseudo Jahn–Teller rules for transition metal systems.

Hybrid-Orbital Approach

The ideas of hybridization and directed valence developed by Pauling and others[35] give surprisingly similar structures (Table IV) to those predicted using eq 5 for several systems. An asterisk labels the structures which are different on the two schemes. For the four-coordinate species the d^0 systems have been shown to be tetrahedral (*e.g.*, VCl_4). Similarly PF_5 is a good example of a d^0 system where the trigonal-bipyramidal structure is observed and not the bizarre pentagonal-pyramidal structure. For the six-coordinate series octahedral geometries are observed for the d^0, d^2, and d^4 hexafluorides. Thus with the sole exception of the five-coordinate 22220 geometry the hybrid-orbital approach gives the same geometries as eq 5 for d^6, d^8, and d^{10} species. Disagreement is limited to the d^0, d^2, and d^4 systems where the hybrid scheme predicts some unusual shapes which are not experimentally observed. The method also does not allow five-coordinate structures with the d^{10} configurations, six-coordinate structures with the d^8 or d^{10} configuration (*i.e.*, the restrictions of the 18-electron rule), or odd-electron species in general.

Discussion

The format of eq 2 and 5 indicates why simple molecular orbital methods may be used to obtain the angular disposition of ligands around a central atom. For the main-group systems, Gavin's simple Hückel approach[7] and, for the transition metal complexes, the calculations by this author[3] using an extended Hückel method have succeeded in a field where theoretical complexity abounds. Equations 2 and 5 suggest that the maximum angular stabilization as determined by central atom–ligand forces is a function purely of the molecular orbital occupation numbers and the spherical harmonics $Y_{lm}(\theta, \phi)$. Thus any simple scheme which calculates overlap integrals as functions of angle should be successful. This structure may be modified somewhat in the transition metal case by lig-

Table IV

		00000	20000	22000	22200	22220	22222
2-coordinate	Hybrid orbitals	d^2 bent	d^2 bent	d^2 bent	d^2 bent	ds bent	sp linear
	This work	Linear*	Linear*	Linear*	Bent	Linear*	Linear
3-coordinate	Hybrid orbitals	d^3 trigonal plane	d^3 trigonal plane	d^3 trigonal plane	d^2p trigonal pyramid	dsp unsym plane	sp^2 trigonal plane
	This work	D_{3h}	D_{3h}	D_{3h}	C_{3v}	C_{2v}(T)	D_{3h}
4-coordinate	Hybrid orbitals	d^4 tetragonal pyramid	d^4 tetragonal pyramid	d^3s tetrahedral	d^2sp irreg tetrahedron	dsp^2 sq planar	sp^3 tetrahedral
	This work	Tetrahedral*	Tetrahedral*	Tetrahedral	Cis divacant	Sq planar	Tetrahedral
5-coordinate	Hybrid orbitals	d^5 pentagonal pyramid	d^4s SPY	d^3sp TBP	d^2sp^2 SPY	d^1sp^3 TBP	
	This work	TBP*	TBP*	TBP	SPY	SPY; see text	
6-coordinate	Hybrid orbitals	d^5s mixed	d^4sp trigonal prism	d^3sp^2 mixed	d^2sp^3 octahedral		
	This work	Octahedral*	Octahedral*	Octahedral*	Octahedral	Octahedral	Octahedral

and–ligand forces which, as we have seen above, with some exceptions take on a secondary role.

The main emphasis in the present scheme for transition metal systems lies with a regime where the most stable geometry is that in which the *unoccupied* d orbitals have the largest net *destabilization*. This is to be contrasted with the usual concept where all *occupied* orbitals have the maximum net *stabilization*. These two standpoints are of course equally valid although from the point of view of calculating the equilibrium geometry the present approach is considerably simpler. For a system in which the central atom is surrounded by n σ ligands the total σ interaction for each of the bonding and antibonding sets is equal to $n\beta_\sigma S_\sigma^2$. Thus for a four-coordinate species with the 220 configuration, for example, in the tetrahedral geometry the destabilization of the d(t_2) set is equal to $^4/_3\beta_\sigma S_\sigma^2$. On distorting the geometry to square planar this degeneracy is split and the destabilization of $d_{x^2-y^2}$ is now $3\beta_\sigma S_\sigma^2$ and that of d_{z^2} is $\beta_\sigma S_\sigma^2$. Thus the square-planar geometry is favored over the tetrahedral for the 220 configuration because either (i) the highest energy d orbital (unoccupied) has a larger destabilization ($3\beta_\sigma S_\sigma^2$ compared with $1.3\beta_\sigma S_\sigma^2$) or (ii) the sum total destabilization energy of the occupied d orbitals is less ($\beta_\sigma S_\sigma^2$ compared with $2.6\beta_\sigma S_\sigma^2$). The behavior of the occupied d orbitals on distortion was used to rationalize qualitatively the minimum internal energy geometry in our previous study.[3] Note that this latter approach is different from one in which the energy change of *all* occupied orbitals (whether predominantly ligand or metal) is considered. The properties of $\Sigma(\sigma)$ in eq 5 readily show the equivalence of all three approaches. The total stabilization of the ligand orbitals is $n\beta_\sigma S_\sigma^2$ irrespective of geometry. The geometry-determining factor is simply the differential destabilization of the system by occupation of metal–ligand antibonding orbitals (predominantly metal d). In contrast to the V.SEPR approach for main-group systems, the present method is also applicable to the geometries of excited electronic states. For example, the cis-divacant structure is suggested for the 200 electronic ground state but a square-planar geometry is predicted for the excited state with a configuration of 110. This applies to both singlet and triplet states; the model only takes orbital occupancy into account. Similarly for the excited state 112, arising from a ground-state configuration 211, the tetrahedral geometry is favored ($\Sigma(\sigma) = 2.7\beta_\sigma S_\sigma^2$) over the cis-divacant ($\Sigma(\sigma) = 1.5\beta_\sigma S_\sigma^2$) and square-planar ($\Sigma(\sigma) = 1.0\beta_\sigma S_\sigma^2$) structures. A knowledge of these excited-state geometries should be of great interest in photochemical studies of transition metal species and as we have noted above is able to rationalize a lot of the photochemistry of $Cr(CO)_5$. This study has centered around binary systems. These have the advantage that the minimum-energy geometry required by eq

5 is independent of the value assigned to β_σ. If MY_nX_m systems are considered, then the relative sizes of the products $S_\sigma(X)\beta_\sigma(X)$ and $S_\sigma(Y)\beta_\sigma(Y)$ need to be included. The applicability of the method to these cases will be discussed separately in another publication.

Finally we may formulate a set of rules with which to predict the angular geometries of these transition metal systems.

(1) Neglect any electrons in the lowest two d orbitals. The *angular* geometry is determined by the occupation numbers of the three highest energy orbitals.

(2) If the occupation numbers are symmetrical (000, 111, or 222), then the VSEPR geometry will be observed.

(3) If a hole exists in the highest energy orbital (220, 221, 210, 110), then the structure will be that of maximum overlap with the lobes of the $d_{x^2-y^2}$ orbital. (A structure intermediate between this geometry and the VSEPR one may be observed for 221.)

(4) If two holes exist symmetrically in the two highest energy orbitals (200, 211, 100), then the structure will be that based on an octahedron containing the maximum number of cis ligands. (A structure intermediate between this geometry and the VSEPR one may be observed for 211.)

For excited-state geometries which are not accommodated in the above discussion (*e.g.*, 112) recourse must be made to calculation of $\Sigma(\sigma)$ by eq 5.

Conclusion

In the preceding sections it has been shown that the "pair repels pair" model of main-group stereochemistry needs to be modified to include the "hole attracts pair" forces which arise from eq 5 when central atom–ligand (specifically in this paper transition metal–ligand) antibonding orbitals are occupied. The hole–pair structures appear to be observed when the energy differences from the regular VSEPR geometry calculated *via* eq 5 are large and should be seen for all three- and four-coordinate species with electron configurations 220, 200, 210, 110, and 100 and five-coordinate species with the configurations 200, 210, and 100. For the configurations 000, 111, and 222 hole–pair forces are independent of angle and the VSEPR structures are observed. For systems where the energy differences between the hole–pair and ligand–ligand structures are small, intermediate geometries are possible, *e.g.*, configurations 221 and 211. For the five-coordinate 220 case where this energy difference is very small, the VSEPR geometry (D_{3h}) is observed accompanied by rapid ligand exchange *via* the most stable hole–pair geometry (C_{4v}).

Appendix. Binomial Expansion of the Secular Determinant

We take the secular determinant $|H_{ij} - S_{ij}E| = 0$ and make the common assumption that $S_{ij} = \delta_{ij}$. Thus for the present case where we consider the interaction between the $d_{x^2-y^2}$ and

d_{z^2} orbitals on the metal with the correct linear combinations of ligand orbitals, the expanded determinant becomes

$$\begin{vmatrix} H_{dd} - E & 0 & H_{d\sigma} & 0 \\ 0 & H_{dd} - E & 0 & H_{d\sigma}' \\ H_{d\sigma} & 0 & H_{\sigma\sigma} - E & 0 \\ 0 & H_{d\sigma}' & 0 & H_{\sigma\sigma} - E \end{vmatrix} = 0 \tag{8}$$

No mixing between the two d orbitals has been allowed to occur.

$H_{d\sigma}$ and $H_{d\sigma}'$ represent the resonance integrals for the interaction of the ligand σ orbitals with the d_{z^2} and $d_{x^2-y^2}$ orbitals. By requiring these resonance integrals to be proportional to the respective overlap integrals (*i.e.*, $H_{d\sigma} = kS_{d\sigma}$), a relationship imposed on the system in the angular-overlap approach, we arrive at the following familiar expression for E

$$E = A \pm (B^2 + k^2 S_{d\sigma}{}^2)^{1/2} \tag{9}$$

where $A = {}^1\!/_2(H_{dd} + H_{\sigma\sigma})$ and $B = {}^1\!/_2(H_{dd} - H_{\sigma\sigma})$. An equation analogous to eq 8 exists for the primed interaction.

Equation 9 may be expanded as a binomial series

$$E = A - B\left[1 + (1/2)\frac{k^2 S_{d\sigma}{}^2}{B^2} - (1/8)\left(\frac{k^2 S_{d\sigma}{}^2}{B^2}\right)^2 + \ldots\right] \tag{10}$$

and combined with the corresponding equation in $S'_{d\sigma}{}^2$ to give the total stabilization energy of these two d orbitals as

$$\Delta E = (1/2)\frac{k^2}{B}\left[S_{d\sigma}{}^2 + S'_{d\sigma}{}^2\right] - (1/8)\frac{k^4}{B^3}\left[S_{d\sigma}{}^4 + S'_{d\sigma}{}^4\right] + \text{terms } [S_{d\sigma}{}^6] \tag{11}$$

The first constant $k^2/2B$ may be identified with β_σ. For the structures based on the octahedron we may write $S_{d\sigma}{}^2 = mS_\sigma{}^2$ and $S'_{d\sigma}{}^2 = (n - m)S_\sigma{}^2$ where n is the number of ligands, which leads to

$$\Sigma(\sigma) = n\beta_\sigma S_\sigma{}^2 - \gamma_\sigma[m^2 + (n - m)^2]S_\sigma{}^4 \tag{12}$$

The leading term is completely analogous to that obtained by the second-order perturbation approach, $\gamma_\sigma = \beta^2/2B$.

For the square-planar geometry ($n = 4$), $m = 3$ and $\Sigma(\sigma)$ $= 4\beta_\sigma S_\sigma{}^2 - 10\gamma_\sigma S_\sigma{}^4$. The corresponding term for the cis-divacant structure ($m = 2.5$) is $4\beta_\sigma S_\sigma{}^2 - 8.5\gamma_\sigma S_\sigma{}^4$. The latter structure is thus favored for the two-hole situation. Similarly

the C_{3v} geometry may be shown to be favored relative to the T shape for such electronic configurations.

References and Notes

(1) R. S. Nyholm and R. J. Gillespie *Quart. Rev., Chem. Soc.*, **11**, 339 (1957); R. J. Gillespie *J. Chem. Educ.*, **40**, 295 (1963).
(2) R. J. Gillespie, "Molecular Geometry," Van Nostrand-Reinhold, New York, N. Y., 1972.
(3) J. K. Burdett, *J. Chem. Soc., Faraday Trans. 2*, **70**, 1599 (1974).
(4) S. F. A. Kettle, *J. Chem. Soc. A*, 420 (1966).
(5) C. E. Schaffer and C. K. Jorgensen, *Mol. Phys.*, **9**, 401 (1964).
(6) C. K. Jorgensen *Struct. Bonding (Berlin)*, **1**, 3 (1966).
(7) R. M. Gavin, *J. Chem. Educ.*, **46**, 413 (1969).
(8) L. S. Bartell, *J. Chem. Educ.*, **45**, 457 (1968).
(9) L. S. Bartell, *Inorg. Chem.*, **5**, 1635 (1966).
(10) L. H. Jones, R. S. McDowell, and M. Goldblatt, *Inorg. Chem.*, **8**, 2349 (1969).
(11) M. Tinkham, "Group Theory and Quantum Mechanics," McGraw-Hill, New York, N. Y., 1964.
(12) R. L. DeKock, *Inorg. Chem.*, **10**, 1205 (1971); H. Huber, E. P. Kundig, M. Moskovitz, and G. A. Ozin, *Can. J. Chem.*, **50**, 2385 (1972); E. P. Kundig, M. Moskovitz, and G. A. Ozin, *ibid.*, **50**, 3587 (1972); J. S. Ogden and J. H. Darling, *J. Chem. Soc., Dalton Trans.*, 1079 (1973).
(13) R. N. Perutz and J. J. Turner, submitted for publication in *J. Amer. Chem. Soc.*
(14) M. Poliakoff and J. J. Turner, *J. Chem. Soc., Dalton Trans.*, 1351 (1973); *ibid.*, 2276 (1974).
(15) O. Crichton, M. Poliakoff, A. J. Rest, and J. J. Turner, *J. Chem. Soc. Dalton Trans.*, 1321 (1973).
(16) G. A. Ozin and A. Vander Voet, *Accounts Chem. Res.*, **6**, 313 (1973).
(17) R. D. Willett, *J. Chem. Phys.*, **41**, 2243 (1964).
(18) B. Morosin and E. C. Lingafelter, *Acta Crystallogr.*, **13**, 807 (1960).
(19) D. C. Bradley and K. J. Fisher, *J. Amer. Chem. Soc.*, **93**, 2058 (1971).
(20) J. K. Burdett, *J. Chem. Soc., Chem. Commun.*, 763 (1973).
(21) G. A. Ozin, unpublished work.
(22) M. Poliakoff, *J. Chem. Soc., Dalton Trans.*, 210 (1974).
(23) D. C. Bradley, M. B. Hursthouse, and P. F. Rodesiler, *Chem. Commun.*, 14 (1969).
(24) H. Mahrike, R. J. Clark, R. Rosanke, and R. K. Sheline, *J. Chem. Phys.*, **60**, 2997 (1974).
(25) M. A. Graham, M. Poliakoff, and J. J. Turner, *J. Chem. Soc. A*, 2939 (1971).
(26) R. N. Perutz and J. J. Turner, *Inorg. Chem.*, in press.
(27) A recent report (E. P. Kundig and G. A. Ozin, *J. Amer. Chem. Soc.*, **36**, 3820 (1974)) of a trigonal-bipyramidal Cr(CO)5 molecule arises through incorrect assignment of infrared bands. See J. K. Burdett, M. A. Graham, M. Poliakoff, R. N. Perutz, A. J. Rest, J. J. Turner, and R. F. Turner, submitted for publication in *J. Amer. Chem. Soc.*
(28) J. K. Burdett, R. N. Perutz, M. Poliakoff, and J. J. Turner, in preparation.
(29) J. K. Burdett, *Inorg. Chem.*, in press.
(30) R. W. Jotham and S. F. A. Kettle, *Inorg. Chim. Acta*, **5**, 183 (1971).
(31) The pyramidal nature of Fe(CO)3 for example discussed above is not rationalized on the basis of the Jahn–Teller approach. The electronic configuration $e''^4a_1{}^2e'^2 = {}^3A_2'$ is not susceptible to Jahn–Teller distortions.
(32) J. K. Burdett, *Appl. Spectrosc. Rev.*, **4**, 43 (1970).
(33) R. G. Pearson, *J. Chem. Phys.*, **52**, 3167 (1970).
(34) J. K. Burdett, *J. Chem. Soc. A*, 1195 (1971).
(35) H. Eyring, J. Walter, and G. E. Kimball, "Quantum Chemistry," Wiley, New York, N. Y., 1944.